PHYSICAL REVIEW C **88**, 011304(R) (2013)

Structure of ^{14}B and the evolution of $N = 9$ single-neutron isotones

S. Bedoor,[1] A. H. Wuosmaa,[1,*] J. C. Lighthall,[1,†] M. Alcorta,[2] B. B. Back,[2] P. F. Bertone,[2,‡] B. A. Brown,[3] C. M. Deibel,[4] C. R. Hoffman,[2] S. T. Marley,[1,2,§] R. C. Pardo,[2] K. E. Rehm,[2] A. M. Rogers,[2] J. P. Schiffer,[2] and D. V. Shetty[1,‖]

[1]*Department of Physics, Western Michigan University, Kalamazoo, Michigan 49008-5252, USA*

[2]*Physics Division, Argonne National Laboratory, Argonne, Illinois 60439, USA*

[3]*Department of Physics and Astronomy, Michigan State University, East Lansing, Michigan 48824, USA*

[4]*Department of Physics and Astronomy, Louisiana State University, Baton Rouge, Louisiana 70803, USA*

(Received 22 April 2013; revised manuscript received 21 June 2013; published 29 July 2013)

We have used the ^{13}B$(d, p)^{14}$B reaction in inverse kinematics to study the properties of states in ^{14}B, the lightest particle-bound $N = 9$ isotone. The spectroscopic information, including spins, parities, and spectroscopic factors for the states observed in ^{14}B are used to deduce the wave functions for the low-lying negative parity $\nu(sd)$ levels, as well as provide information about the evolution of the effective neutron $1s_{1/2} - 0d_{5/2}$ single-particle energies. The data confirm that the ground and first-excited states are predominantly s wave in character and are single-neutron halo states. The effective single-particle energies are found to match the trends set by other $N = 9$ isotones.

DOI: 10.1103/PhysRevC.88.011304 PACS number(s): 21.10.Jx, 25.45.Hi, 25.60.Je, 27.20.+n

The nucleus ^{14}B, with a ground-state neutron-separation energy of 0.969 MeV, is the lightest $N = 9$ isotone that is particle bound. ^{14}B thus presents an opportunity to study the evolution of the properties of single-neutron states in the *sd* shell at the limits of stability. In light nuclei, the behavior of the single-particle orbitals is indicative of many phenomena observed in heavier nuclei; for instance, those induced by the tensor force [1–3] and the effective single-particle energies (ESPE) are important ingredients in shell-model calculations. For $N = 9$, it is well known that between ^{17}O and ^{15}C, the neutron single-particle $1s_{1/2}$ and $0d_{5/2}$ orbitals are inverted, due in large part to the emptying of the proton $0p_{1/2}$ orbital. It is interesting to determine how these energies evolve beyond ^{15}C. To construct the wave functions for states in ^{14}B and determine the $1s_{1/2}$ and $0d_{5/2}$ ESPE, it is necessary to obtain spectroscopic information, including neutron spectroscopic factors. Such information may be gathered from the ^{13}B$(d, p)^{14}$B neutron-adding reaction. Here, we report the results of a study of this reaction in inverse kinematics performed using the Helical Orbit Spectrometer (HELIOS) at Argonne National Laboratory.

Extracting information about ^{14}B involves untangling the coupling of the *sd*-shell neutrons to the $3/2^-$ ground state of ^{13}B. This coupling leads to a $(1,2)^-$ doublet for $\pi(0p_{3/2})^{-1}\nu(1s_{1/2})$, and $(1,2,3,4)^-$ and $(0,1,2,3)^-$ multiplets for neutron $0d_{5/2}$ and $0d_{3/2}$ states, respectively. Configuration mixing between states with the same spin and parity in ^{14}B is possible, especially for the neutron $1s_{1/2}$ and $0d_{5/2}$ orbitals where that splitting may be small as suggested by the separation between the ground $(1/2^+)$ and first-excited $(5/2^+, E_X = 0.74$ MeV) states in ^{15}C [4]. The $0d_{3/2}$ $3/2^+$ state in ^{15}C is at a high excitation energy (4.8 MeV) and $0d_{3/2}$ neutrons are unlikely to play a role at low energies in ^{14}B. Other states that could produce admixtures might arise from a $1/2^-$ state in ^{13}B, tentatively associated with a 3.71 MeV excitation [5], made by promoting a proton out of the $0p_{3/2}$ orbital. Coupled to a $1s_{1/2}$ or $0d_{5/2}$ neutron, this would give rise to $(0, 1)^-$ and $(2, 3)^-$ doublets, but the admixtures to states strongly populated in (d,p) should be small. Finally, while neutron p-wave configurations have been shown to play a role in the structure of ^{12}Be [6–9], it appears that in ^{13}Be [10–12] and ^{14}Be [13], neutron *s*-*d* shell configurations dominate, and we expect that to be the case for states in ^{14}B formed by neutron addition.

Rather little is known experimentally about ^{14}B; the inset in Fig. 1 shows a level diagram from Ref. [4]. Most spin-parity assignments for negative-parity states were obtained from a study of the ^{14}C$(^7$Li,^{7}Be$)^{14}$B reaction and a comparison of the experimental spectrum from that reaction with the known level structure of ^{12}B [14]. An excited 2^- state was reported in that work at 1.82 MeV, which was later associated with a broad ($\Gamma \approx 1$ MeV) 2^- excitation populated in the ^{14}C$(\pi^-, \gamma)^{14}$B reaction at $E_X = 2.15$ MeV [15]; compilations [4] place this state at 1.86 ± 0.07 MeV. Neutron knockout reactions from ^{14}B also support an s-wave dominated 2^- ^{14}B ground state [16,17]. Positive-parity states in ^{14}B have been studied through ^{14}Be β decay [18] and charge-exchange reactions [19]; these will not be populated in (d, p). Additional information can be inferred from data for the mirror nucleus ^{14}F, which has been studied recently using resonant ^{13}O $+ p$ scattering [20]. There, four resonances corresponding to the mirrors of the $(2,1,3,4)^-$ states in ^{14}B were observed, with the $(2,1)^-$ states being dominated by $\ell = 0$, and the $(3,4)^-$ levels being pure $\ell = 2$. The mirror to a broad excited 2^- state was not observed in that work. Sherr and Fortune have analyzed the results of the ^{14}F work and used them to deduce model excitation energies, spectroscopic factors, and reduced widths for states in ^{14}B [21].

The nucleus ^{14}B has been the subject of early shell-model calculations by Millener and Kurath (MK) [1], and

*Corresponding author: alan.wuosmaa@wmich.edu

†Present address: TRIUMF, Vancouver, BC V6T 2A3, Canada.

‡Present address: Marshall Space Flight Center, Huntsville, AL 35811, USA.

§Present address: University of Notre Dame, South Bend, IN 46558, USA.

‖Present address: Grand Valley State University, Allendale, MI 49401, USA.

TABLE I. Experimental and theoretical excitation energies and neutron spectroscopic factors for states in ^{14}B. Experimental spectroscopic factors are normalized to $S(3^-) = 1.0$ and the uncertainties are (fit)(theory). Experimental excitation energies are from Ref. [4] unless otherwise indicated.

State	E_X (MeV)					S_{expt}		S_{WBP}		S_{WBT}	
	Expt.	WBP	WBT	YUAN[a]	NCSM[b]	$S_{\ell=0}$	$S_{\ell=2}$	$S_{\ell=0}$	$S_{\ell=2}$	$S_{\ell=0}$	$S_{\ell=2}$
2_1^-	0.00	0.00	0.00	0.00	0.00	0.71(5)(14)	0.17(5)(4)	0.64	0.31	0.66	0.29
1_1^-	0.654(9)[c]	0.90	1.19	0.70	1.4	0.94(20)(20)	$\leqslant$0.06	0.85	0.10	0.86	0.10
3_1^-	1.38(3)	1.17	1.48	1.50	1.4		$\equiv$1.00		0.96		0.98
2_2^-	1.86(7)	1.62	2.05	1.95	3.3	[0.17(5)(4)][d]	[0.71(5)(20)][d]	0.33	0.59	0.31	0.58
4_1^-	2.08(5)	1.12	1.74	2.40	3.1		1.00(10)(20)		0.95		0.96
(1_2^-)	4.5[e]	4.5	4.86		5.9	[$\leqslant$0.06][d]	[0.94(20)(20)][d]	0.12	0.64	0.13	0.67

[a]From Ref. [22].
[b]From Ref. [23].
[c]Value from Ref. [30].
[d]Calculated as described in the text.
[e]Assumed value as described in the text.

more modern interactions have been applied to the mirror nucleus ^{14}F [20]. The MK interaction gave a sequence of $(2,3,4,1)^-$ and suggested s-wave dominated 2_1^- and 1_1^- states, with configuration mixing limited to the 2^- levels. Later shell-model calculations described below and calculations for ^{14}F given in [20] predict a negative-parity sequence of $(2,1,3,4)^-$. All of these later calculations place the 2_2^- state above the 4_1^- level and predict the 1_2^- state to lie between 1 and 3 MeV above the 4^- excitation. A recent calculation from Yuan *et al.* [22] better reproduces the experimental level ordering and spacing (see Table I). *Ab-initio* calculations done with the no-core shell model (NCSM) have also produced excitation energies for ^{14}B [23]. There, differences between the calculated and observed spectrum were attributed to possible deficiencies in the nucleon-nucleon interaction, or the neglect of three-body forces.

We have studied the ^{13}B$(d, p)^{14}$B reaction in inverse kinematics using a secondary beam of ^{13}B ions ($T_{1/2} =$ 17.33 ms) from the Argonne Tandem-Linac Accelerator System (ATLAS) in-flight facility [24] at Argonne National Laboratory. The ^{13}B beam was produced by proton removal from a ^{14}C primary beam using the ^{9}Be(^{14}C,^{13}B)^{10}B reaction. The energy and intensity of the ^{14}C beam were 240 MeV and 80 to 100 pnA, respectively, and the production target was a 15 mg/cm^2 thick ^{9}Be foil. The high bombarding energy was chosen to improve the cross section of the production reaction due to its very negative Q value of -14.246 MeV. The ^{13}B beam had an energy of 204 MeV and an energy spread of 5 MeV resulting from the kinematics of the production reaction and straggling in the production target. The beam-spot size of less than a 5 mm $\times$ 5 mm square defined by a collimator at the end of the silicon-detector array does not affect the resolution properties of HELIOS. The ^{13}B intensity was between 2×10^4 and 4×10^4 particles per second. Events from small impurities in the ^{13}B beam from lower charge states of ^{14}C ($\approx$30%) and ^{10}Be ($\approx$10%) were eliminated by requiring a coincidence between protons and identified ^{13,14}B reaction products as described below. The ^{13}B flux and the beam composition were monitored using a silicon surface-barrier $\Delta E - E$ telescope placed on the beam axis. A 0.5 mm thick Ta attenuator placed in front of the 0° telescope reduced the beam flux in the monitor detector by a factor of 100, limiting the count rate to a manageable value.

Protons were detected using HELIOS [25,26]. The experimental arrangement was similar to that used in other studies of (d, p) reactions in inverse kinematics with light, radioactive beams, including ^{12}B$(d, p)^{13}$B [27], ^{15}C$(d, p)^{16}$C [28], and ^{19}O$(d, p)^{20}$O [29]. In HELIOS, particles are transported in helical orbits from the target to an array of position-sensitive silicon detectors by a uniform, 2.85 T magnetic field oriented parallel to the beam direction. The silicon-detector array was positioned upstream of the target corresponding to laboratory angles greater than 90°, covering between $-450 \leqslant z \leqslant -90$ mm, where z is the distance between the target and the point at which the protons return to the solenoid axis. The recoiling ^{14,13}B nuclei from the population of bound or unbound states in ^{14}B were identified in coincidence with the protons using an additional set of four silicon $\Delta E - E$ telescopes subtending laboratory polar angles from 0.5° to 2.8° and 92% of the available azimuthal angle range. The ^{13}B beam bombarded a $(CD_2)_n$ foil with an areal density of 220 μg/cm^2. All events with a particle detected in the HELIOS silicon-detector array, as well as additional down-scaled samples of singles events from the recoil-detector and 0°-monitor telescopes, were recorded. Calibration information for the HELIOS silicon-detector array was obtained from α-particle sources and measurements with the primary ^{14}C beam.

The measured excitation-energy spectrum for the ^{13}B$(d, p)^{14}$B reaction appears in Fig. 1. The filled(open) histogram represents events obtained with protons in coincidence with identified ^{14}B(^{13}B) ions. The excitation-energy resolution of 220 keV full width at half maximum (FWHM) is dominated by the energy spread of the ^{13}B beam. Random coincidences between particles in the HELIOS silicon array and recoil-detector telescopes were subtracted using timing measurements between those devices. Four narrow peaks are observed, which we associate with the 2_1^-, (1_1^-), (3_1^-), and (4_1^-) excitations. The excitation energies are in agreement with the literature values except for the first-excited state, which, while given in Ref. [4] as 740 $\pm$ 40 keV, in our measurement agrees

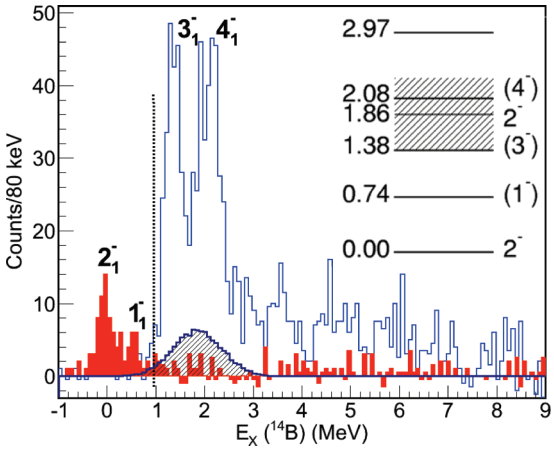

FIG. 1. (Color online) ^{14}B excitation-energy spectrum from the ^{13}B(d, p)^{14}B reaction. The filled (open) histogram corresponds to protons detected in coincidence with identified ^{14}B(^{13}B) recoil ions. The vertical dashed line shows the neutron-separation energy, and the cross-hatched peak is described in the text. The inset shows the level diagram for ^{14}B from [4].

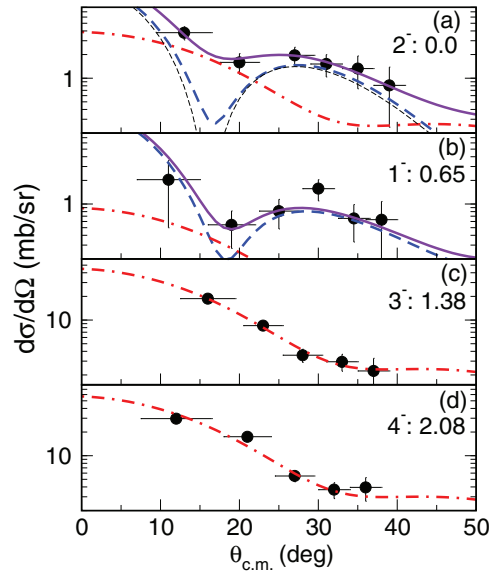

FIG. 2. (Color online) Angular distributions for different states in the ^{13}B(d, p)^{14}B reaction. The horizontal bars represent the angular range for each data point. The curves represent DWBA calculations described in the text, with the thick-dashed, dot-dashed, and solid curves corresponding to $\ell = 0$, 2, and $0 + 2$, respectively. The thin-dashed curve in (a) shows the $\ell = 0$ result for the 2^-_1 state before averaging over the scattering angle.

with the $E_X(1^-_1) = 654 \pm 9$ keV suggested by gamma-ray observations [30]. The width of the 3^-_1 peak at 1.38 MeV is comparable to our instrumental resolution, though the 4^-_1 peak is broader ($\Gamma \approx 300$ keV), suggesting that we are sensitive to the natural width of that level. Deconvoluting the experimental resolution, we estimate that the width of the 4^-_1 state is roughly $\Gamma \approx 200 \pm 50$ keV. We cannot rule out a contribution from the broad reported 2^-_2 state; however we are probably insensitive to this excitation due to its width and expected yield. The cross-hatched histogram in Fig. 1 represents an estimate of how this state would appear in our data, and it would likely be obscured by the peaks from the much stronger 3^-_1 and 4^-_1 transitions. At excitation energies greater than 2 MeV, the spectrum is dominated by broad resonances. We do not see evidence of a broad state observed in the ^{14}Be(p, n)^{14}B reaction at 4.06 MeV, tentatively assigned 3^+ or 3^- [19].

Figure 2 shows angular distributions obtained for the four low-lying narrow states in ^{14}B populated in the (d, p) reaction. The cross sections were obtained from the yields in the silicon-array detectors, with the total number of beam particles determined from the yield in the 0°-monitor detector. The proton yields were corrected for the solid-angle acceptance of the silicon-detector array, and the recoil-coincidence efficiency for the beam-like ^{13,14}B reaction partners detected at forward angles. The recoil-coincidence efficiency was determined from Monte-Carlo simulations of particle transport in HELIOS for the two- and three-body final states where appropriate, as described in [26]. Systematic uncertainties from the Monte-Carlo simulations arising from the effects of possible detector misalignment were approximately 10%. Due to the beam attenuator, the measurement of the integrated beam flux depended on the beam spot size and shape, and the sensitivity of the absolute normalization to those effects has also been investigated with Monte-Carlo simulations. We estimate that the total uncertainty in the absolute cross-section scale is approximately 30%.

The curves in Fig. 2 represent the results of distorted-wave Born-approximation (DWBA) calculations calculated using the finite-range code PTOLEMY [31]. The optical-model parameters for the entrance and exit channels were taken from Refs. [32] and [33], and reproduce d+^{12}C and p+^{12}C elastic scattering at $E_d = 30$ and $E_p = 15$ MeV. The bound-state form factors were obtained from a Woods-Saxon well with radius parameter $r_0 = 1.2$ fm and diffuseness $a = 0.6$ fm, and depth adjusted to match the known neutron binding energy. For the unbound 3^-_1 and 4^-_1 states, the form factors were calculated with the approximation that the states were bound by 100 keV.

Additional calculations using the code DWUCK4 [34], which implements the method of Vincent and Fortune [35] for unbound final states, give variations in the average $\ell = 2$ cross section in the angle range of interest of ≈10% moving from $E_X = 0.9$ MeV (bound) to $E_X = 2.0$ MeV (unbound). Variations in the DWBA results for changes in the bound-state well parameters of 5% in r_0 and 20% in a lead to changes in the ratio of $\sigma(\ell = 0)/\sigma(\ell = 2)$ of approximately 20% over the measured angular range. Also, the angular-distribution shapes are nearly identical to those obtained using a theory that includes the effect of deuteron breakup for the ^{16}O(d, p)^{17}O reaction at similar deuteron energies [36]. We use these variations as an estimate of the theoretical systematic uncertainty on the spectroscopic factors discussed below.

The calculations have been averaged over an angular range corresponding to the angular acceptance for the data points. For the ground- and first-excited states that are assigned 2^- and 1^-, respectively, both $\ell = 0$ and 2 neutron transfers are permitted. For those two states, the thick-dashed, dot-dashed,

and solid curves in Figs. 2(a) and 2(b) correspond to results obtained from $\ell = 0, 2$, and the sum of contributions for $\ell = 0$ and 2, respectively, where the amounts of $\ell = 0$ and 2 have been adjusted to produce a best fit to the data. The $\ell = 0$ curve for the 2_1^- state before averaging over the angle appears as the thin-dashed curve in Fig. 2(a); the $\ell = 2$ curves do not change appreciably with averaging. The angular distributions for the 3_1^- and 4_1^- levels are consistent with pure $\ell = 2$ transitions, consistent with their suggested spin assignments.

Relative spectroscopic factors S_ℓ for each state were obtained following the usual prescription that S_ℓ is given by the ratio of the experimental to the calculated DWBA cross section. Due to the uncertainties from the absolute normalization, we report relative values for comparison between the transitions to different states. The normalization scale for the S_ℓ was set by assigning the spectroscopic factor for the transition to the suggested 3_1^- state at 1.38 MeV $S_2(3_1^-) \equiv 1.00$. With this normalization, the ℓ values and spectroscopic factors support the tentative spin assignments in the literature for all four narrow levels populated in the present reaction.

Table I lists the values for the resulting spectroscopic factors. The uncertainties are from the fitting procedure and estimates of the theoretical systematic uncertainty. The ground state is predominantly $\ell = 0$, with an approximate 20% admixture of $\ell = 2$. The 1^- first-excited state is, within uncertainties, pure $\ell = 0$. Table I also shows the spectroscopic factors predicted from shell-model calculations using two different interactions, WBP and WBT [37], as well as the predicted energies of the four narrow states. The agreement between the measured and calculated spectroscopic factors from both the WBP and WBT interactions is excellent. For the 3_1^- and 4_1^- states, the shell-model values are both close to unity; from the data the spectroscopic factor for the 4_1^- state is equal within uncertainties to the assumed value of 1.0 for the 3_1^- state. With $S_2(4_1^-) \approx 1$, the width expected for the 4_1^- level is approximately Γ =200 keV, also in agreement with the experimentally deduced value.

The spectroscopic factors may be compared with the sum-rule values of Macfarlane and French [38]. For neutron-adding reactions, the number of holes in a shell j is given by

$$G_+(j) = \sum_k \frac{(2J_f + 1)_k}{(2J_i + 1)} (S_{\ell j})_k, \tag{1}$$

where the summation is over the states k with given values of ℓ and j, j is the total angular momentum for a given orbital, and J_i and J_f are the initial and final spins. $(S_{\ell j})_k$ represents the spectroscopic factor for the state k with quantum numbers ℓ and j. Including the four observed narrow states, the experimental values of $G_+(j)$ are 1.6 ± 0.2 $(1s_{1/2})$ and 4.3 ± 0.3 $(0d_{5/2})$. The sum rule demands that for each J_f the total $S = 1$, and the values of G_+ are 2 and 6 for $1s_{1/2}$ and $0d_{5/2}$, respectively. These results indicate that, as expected, some strength is missing for both orbitals in the states seen in the experiment.

We can estimate the additional strength from the unobserved 2_2^- and 1_2^- states by ignoring the $0d_{3/2}$ orbital, and assuming that the pairs of 2^- and 1^- levels are formed by orthogonal combinations of $1s_{1/2}$ and $0d_{5/2}$ configurations. The wave functions for these states are then given by

$$\begin{aligned} |J_1^-\rangle &= \alpha_J \nu(1s_{1/2}) + \beta_J \nu(1d_{5/2}), \\ |J_2^-\rangle &= -\beta_J \nu(1s_{1/2}) + \alpha_J \nu(1d_{5/2}), \end{aligned} \tag{2}$$

where $J = 2$ and 1, and the values of α_J and β_J are determined from the relative $\ell = 0$ and 2 spectroscopic factors for the ground- and first-excited states. If we include the additional contributions for the 2_2^- and 1_2^- states, the resulting numbers of $1s_{1/2}$ and $0d_{5/2}$ holes are 1.9 ± 0.2 and 5.9 ± 0.3, respectively, very close to the sum-rule values. For comparison, the corresponding values from shell-model calculations with the WBP(WBT) interactions, including the lowest six states, are 1.94(1.95) for $1s_{1/2}$ and 5.50(5.54) for $0d_{5/2}$.

If excitation energies and spectroscopic strengths for all the relevant states are available, the ESPE are given by the centroid:

$$E_0(j) = \sum_k \frac{(2J + 1)_k (S_{\ell j})_k E_k}{(2J + 1)_k (S_{\ell j})_k}, \tag{3}$$

where the sum is over all excited states, $E_0(j)$ is the ESPE, $(S_{\ell j})_k$ and E_k are the spectroscopic factor and excitation energy for the state k, respectively. This formulation is equivalent to that given in Ref. [39]. We do not determine the excitation energies of the 2_2^- and 1_2^- states. For the purposes of this discussion, we assume that the 2_2^- state is the broad excitation at 1.86 MeV reported in the literature [4], and we assign the WBP excitation energy of 4.50 MeV to a hypothetical 1_2^- level. We emphasize that this latter choice is made only for the sake of argument, and that the energy of the 1_2^- state remains unknown. Under these assumptions, the values for $E_0(1s_{1/2})$ and $E_0(0d_{5/2})$ are 0.5 ± 0.1 MeV, and 2.0 ± 0.4 MeV, respectively. The uncertainties include those of the spectroscopic factors, as well as an uncertainty of 2 MeV in the value of the excitation energy for the 1_2^- state. The energies of the 2_2^- and 1_2^- states actually have only a small influence on the results; for $1s_{1/2}$ this is due to the small $\ell = 0$ spectroscopic factors, and for $0d_{5/2}$ the 2_2^- and 1_2^- states carry little weight due to the $2J + 1$ statistical factor that strongly enhances the contributions of the 3_1^- and 4_1^- excitations.

Figure 3 shows the trends of the $1s_{1/2}$ and $0d_{5/2}$ ESPE in $N = 9$ isotones from ^{17}O to ^{13}Be, expressed relative to the one-neutron separation energy. For ^{17}O and ^{15}C, the values

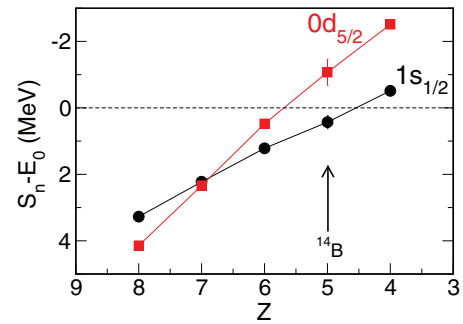

FIG. 3. (Color online) Effective single-particle binding energies of the $1s_{1/2}$ and $0d_{5/2}$ orbitals as a function of Z, for $N = 9$ isotones. The ^{14}B points are from the present measurement, and the lines are to guide the eye.

are from the excitation energies of the lowest $1/2^+$ and $5/2^+$ states, for ^{16}N we use the excitation energies weighted by the spectroscopic factors given in Ref. [40], and for ^{13}Be, values have been reported from studies of neutron knockout from ^{14}Be by Simon *et al.* [12]. The results for ^{14}B fit extremely well with the trends established by the other nearby $N = 9$ isotones.

In summary, we have studied neutron single-particle states in the $N = 9$ isotone ^{14}B with the ^{13}B$(d, p)^{14}$B reaction. The $\ell = 0$ and 2 spectroscopic factors for the narrow 2^-_1, 1^-_1, 3^-_1, and 4^-_1 levels are in good agreement with the predictions of shell-model calculations, and suggest moderate $1s_{1/2} - 0d_{5/2}$ configuration mixing for low-lying 2^- states. The 1^-_1 first-excited state is nearly pure $1s_{1/2}$, and with a neutron-binding energy of only 313 keV is one of the best known examples of a single-neutron halo state. Using some simple assumptions about the structures of the unobserved 2^-_2 and 1^-_2 states, we have estimated the $1s_{1/2}$ $0d_{5/2}$ ESPE which fit extremely well within the trends established for other $N = 9$ isotones. This last result depends on the excitation energies of the unobserved states, and it is possible that more information about these excitations might be obtained from other reactions populating ^{14}B.

This work was supported by the US Department of Energy, Office of Nuclear Physics, under Contracts No. DE-FG02-04ER41320 and No. DE-AC02-06CH11357, and the US National Science Foundation under Grant No. PHY-1068217.

[1] D. J. Millener and D. Kurath, Nucl. Phys. A **255**, 315 (1975).
[2] Takaharu Otsuka *et al.*, Phys. Rev. Lett. **87**, 082502 (2001).
[3] T. Otsuka, T. Suzuki, R. Fujimoto, H. Grawe, and Y. Akaishi, Phys. Rev. Lett. **95**, 232502 (2005).
[4] F. Azjenberg-Selove, Nucl. Phys. A **523**, 1 (1991).
[5] G. Mairle and G. J. Wagner, Nucl. Phys. A **253**, 253 (1975).
[6] A. Navin *et al.*, Phys. Rev. Lett. **85**, 266 (2000).
[7] H. Iwasaki *et al.*, Phys. Lett. B **481**, 7 (2000).
[8] H. Iwasaki *et al.*, Phys. Lett. B **491**, 8 (2000).
[9] S. Shimoura *et al.*, Phys. Lett. B **560**, 31 (2003).
[10] M. Thoennessen, S. Yokoyama, and P. G. Hansen, Phys. Rev. C **63**, 014308 (2000).
[11] H. Simon *et al.*, Nucl. Phys. A **734**, 323 (2004).
[12] H. Simon *et al.*, Nucl. Phys. A **791**, 267 (2007).
[13] M. Labiche *et al.*, Phys. Rev. Lett. **86**, 600 (2001).
[14] G. C. Ball *et al.*, Phys. Rev. C **33**, 395 (1973).
[15] Helmut W. Baer *et al.*, Phys. Rev. C **28**, 761 (1983).
[16] D. Bazin *et al.*, Phys. Rev. C **57**, 2156 (1998).
[17] V. Guimarães *et al.*, Phys. Rev. C **61**, 064609 (2000).
[18] N. Aoi *et al.*, Phys. Rev. C **66**, 014301 (2002).
[19] Y. Satou *et al.*, Phys. Lett. B **697**, 459 (2011).
[20] V. Z. Goldberg *et al.*, Phys. Lett. B **692**, 307 (2010).
[21] R. Sherr and H. T. Fortune, Phys. Lett. B **699**, 281 (2011).
[22] C. Yuan, T. Suzuki, T. Otsuka, F. Xu, and N. Tsunoda, Phys. Rev. C **85**, 064324 (2012).
[23] P. Maris, A. M. Shirokov, and J. P. Vary, Phys. Rev. C **81**, 021301(R) (2010).
[24] B. Harss *et al.*, Rev. Sci. Instrum. **71**, 380 (2000).
[25] A. H. Wuosmaa *et al.*, Nucl. Instrum. Methods Phys. Res. A **580**, 1290 (2007).
[26] J. C. Lighthall *et al.*, Nucl. Instrum. Methods Phys. Res. A **622**, 97 (2010).
[27] B. B. Back *et al.*, Phys. Rev. Lett. **104**, 132501 (2010).
[28] A. H. Wuosmaa *et al.*, Phys. Rev. Lett. **105**, 132501 (2010).
[29] C. R. Hoffman *et al.*, Phys. Rev. C **85**, 054318 (2012).
[30] R. Kanungo *et al.*, Phys. Lett. B **608**, 206 (2005).
[31] M. H. Macfarlane and S. C. Pieper, Argonne National Laboratory Report No. ANL-76-11, Rev. 1, 1978 (unpublished).
[32] H. Ohnuma *et al.*, Nucl. Phys. A **448**, 205 (1986).
[33] J. S. Petler, M. S. Islam, R. W. Finlay, and F. S. Dietrich, Phys. Rev. C **32**, 673 (1985).
[34] P. D. Kunz (unpublished).
[35] C. M. Vincent and H. T. Fortune, Phys. Rev. C **2**, 782 (1970).
[36] N. K. Timofeyuk and R. C. Johnson, Phys. Rev. C **59**, 1545 (1999).
[37] E. K. Warburton and B. A. Brown, Phys. Rev. C **46**, 923 (1992).
[38] M. H. Macfarlane and J. B. French, Rev. Mod. Phys. **32**, 567 (1960).
[39] M. Baranger, Nucl. Phys. A **149**, 225 (1970).
[40] W. Bohne *et al.*, Nucl. Phys. A **196**, 41 (1972).